



Differential effects of Wnt- β -catenin signaling in Purkinje cells and Bergmann glia in spinocerebellar ataxia type 1

Kimberly Luttik^{a,b}, Leon Tejwani^{a,b,1}, Hyoungseok Ju^{c,2}, Terri Driessen^c, Cleo J. L. M. Smeets^c, Chandrakanth Reddy Edamakanti^d, Aryaan Khan^e, Joy Yun^e, Puneet Opal^d, and Janghoo Lim^{a,b,c,f,g,3}

Edited by Hugo Bellen, Baylor College of Medicine, Houston, TX; received May 23, 2022; accepted June 25, 2022

Spinocerebellar ataxia type 1 (SCA1) is a dominantly inherited neurodegenerative disease characterized by progressive ataxia and degeneration of specific neuronal populations, including Purkinje cells (PCs) in the cerebellum. Previous studies have demonstrated a critical role for various evolutionarily conserved signaling pathways in cerebellar patterning, such as the Wnt- β -catenin pathway; however, the roles of these pathways in adult cerebellar function and cerebellar neurodegeneration are largely unknown. In this study, we found that Wnt- β -catenin signaling activity was progressively enhanced in multiple cell types in the adult SCA1 mouse cerebellum, and that activation of this signaling occurs in an ataxin-1 polyglutamine (polyQ) expansion-dependent manner. Genetic manipulation of the Wnt- β -catenin signaling pathway in specific cerebellar cell populations revealed that activation of Wnt- β -catenin signaling in PCs alone was not sufficient to induce SCA1-like phenotypes, while its activation in astrocytes, including Bergmann glia (BG), resulted in gliosis and disrupted BG localization, which was replicated in SCA1 mouse models. Our studies identify a mechanism in which polyQ-expanded ataxin-1 positively regulates Wnt- β -catenin signaling and demonstrate that different cell types have distinct responses to the enhanced Wnt- β -catenin signaling in the SCA1 cerebellum, underscoring an important role of BG in SCA1 pathogenesis.

spinocerebellar ataxia type 1 | neurodegeneration | Wnt- β -catenin signaling | Purkinje cells | Bergmann glia

Spinocerebellar ataxia type 1 (SCA1) is an adult-onset neurodegenerative disorder caused by a trinucleotide repeat expansion of a glutamine-encoding CAG tract in *ATXN1* (1). In SCA1, specific neuronal populations degenerate at later stages of disease, including cerebellar Purkinje cells (PCs), brainstem cranial nerve nuclei, and inferior olive neurons (2). Although ataxia-related motor changes typically manifest during adulthood, animal models of SCA1 have revealed substantial molecular and circuit-level alterations in the cerebellum at time points prior to the onset of robust behavioral deficits (3–8), suggesting developmental abnormalities can contribute to long-term cerebellar health and SCA1 pathogenesis. Furthermore, although *ATXN1* is ubiquitously expressed throughout the brain (9–11), the cellular and molecular mechanisms leading to the selective degeneration of specific cell types is largely unknown.

Among the different signaling pathways that have been identified through unbiased profiling of ataxia animal models, several studies suggest that components of the Wnt signaling pathway are perturbed in SCA1 and other forms of ataxia, with ataxin-1- and ataxin-3-null mice exhibiting altered expression of genes involved in the Wnt signaling pathway (8, 12–14). The Wnt signaling pathway is comprised of three highly conserved signal transduction pathways: the canonical Wnt- β -catenin pathway, and the noncanonical Wnt-planar cell polarity and Wnt-calcium pathways (15). Within the cerebellum, the canonical Wnt- β -catenin pathway plays crucial roles in regulating the proliferation, migration, and differentiation of diverse cell types during cerebellar morphogenesis (16–23). Previous studies have shown that aberrant activation of Wnt- β -catenin signaling in cerebellar granule precursor cells can inhibit their proliferation, prompting precocious differentiation during development (21). Additionally, a number of genes encoding key components in the Wnt- β -catenin signaling pathway—including *Apc*, *Gsk3 β* , *Ctnnb1* (encoding β -catenin), and *Lef-1*—as well as its target genes, including *Cend1* and *Myc*, are expressed in adult PCs (9, 24, 25). Together, these studies indicate that Wnt- β -catenin signaling is active and is homeostatically regulated in the cerebellum during development and into adulthood. Thus, although it is clear that Wnt plays a fundamental role in establishing proper cerebellar cytoarchitecture, the precise physiological role of persistent Wnt signaling in different cell types of the adult cerebellum remains elusive. Furthermore, the nature of Wnt- β -catenin signaling

Significance

The mechanisms underlying the degeneration of specific cellular populations in various neurodegenerative disorders remain unknown. Here, we show that the polyQ expansion of ataxin-1 activates the Wnt- β -catenin signaling pathway in various cell types, including Purkinje cells and Bergmann glia, in the cerebellum of spinocerebellar ataxia type 1 (SCA1) mouse models. We used conditional mouse genetics to activate and silence this pathway in different cell types and found elevated activity of this signaling pathway impacted Bergmann glia and Purkinje cell populations differently. This study highlights the important role of the Wnt- β -catenin signaling pathway in glial cell types for SCA1 pathogenesis.

Author contributions: K.L., L.T., H.J., and J.L. designed research; K.L., L.T., H.J., T.D., C.J.L.M.S., C.R.E., A.K., J.Y., and P.O. performed research; K.L., L.T., H.J., T.D., C.J.L.M.S., A.K., and J.Y. analyzed data; and K.L., L.T., and J.L. wrote the paper.

The authors declare no competing interest.

This article is a PNAS Direct Submission.

Copyright © 2022 the Author(s). Published by PNAS. This article is distributed under Creative Commons Attribution-NonCommercial-NoDerivatives License 4.0 (CC BY-NC-ND).

¹Present address: Denali Therapeutics Inc., South San Francisco, CA 94080.

²Present address: Translational Biology, Evotec SE, 22419 Hamburg, Germany.

³To whom correspondence may be addressed. Email: janghoo.lim@yale.edu.

This article contains supporting information online at <http://www.pnas.org/lookup/suppl/doi:10.1073/pnas.2208513119/-/DCSupplemental>.

Published August 15, 2022.

perturbation and the functional implications of this dysregulation in the SCA1 cerebellum at various stages of disease are unclear.

In this study, we demonstrate that Wnt- β -catenin signaling is activated in multiple cerebellar cell types in an age-dependent manner in vivo in SCA1 through both cell-autonomous and noncell-autonomous mechanisms. We identified a molecular mechanism through which ataxin-1 positively regulates Wnt- β -catenin signaling in an polyglutamine (polyQ)-dependent manner to cell autonomously enhance Wnt target gene expression in PCs. Interestingly, expression of polyQ-expanded ataxin-1 specifically in PCs also resulted in increased production of multiple secreted Wnt ligands and higher Wnt activity in other cell populations, including Bergmann glia (BG). To understand the impact of Wnt signaling in these different cerebellar cell types, we used conditional mouse genetics approaches to manipulate levels of Wnt- β -catenin signaling in a cell-type-specific manner in SCA1 mouse models. Our data revealed differential effects of Wnt- β -catenin signaling in different cell types, with perturbations in Wnt signaling in BG having a greater impact on overall cerebellar health than in PCs. Taken together, these data describe the effect of altering Wnt signaling in different cell types in the adult cerebellum and support a role for BG in the progressive cerebellar dysfunction observed in SCA1.

Results

Wnt- β -Catenin Signaling Is Enhanced in the SCA1 Cerebellum.

Due to the well-defined role of Wnt- β -catenin signaling (Fig. 1*A*) in cerebellar circuit formation (16–23), and the involvement of developmental changes in long-term cerebellar health in SCA1 (4, 5), we sought to interrogate if and how Wnt- β -catenin signaling is involved in SCA1 at various stages of disease progression. To this end, we first examined Wnt- β -catenin signaling in SCA1 knockin (KI) mice that express *Atnx1* containing 154 CAG repeats under the control of its endogenous promoter (*Atnx1*^{154Q/2Q}; SCA1 KI) (26). Gene expression of Wnt- β -catenin target genes *Ccnd1* and *c-Myc* was progressively up-regulated in vivo in the SCA1 KI cerebellum in an age-dependent manner, with significantly elevated expression at 30 wk but not at 6 wk (Fig. 1*B*). Interestingly, we found that this elevation of Wnt- β -catenin target genes was not observed in the cortex of SCA1 KI mice (*SI Appendix*, Fig. S1), suggesting that enhanced Wnt- β -catenin signaling occurs distinctively in brain regions affected in SCA1. Furthermore, protein levels of active β -catenin were also elevated in an age-dependent manner in the SCA1 KI cerebellum (*SI Appendix*, Fig. S2). Together, these data suggest that Wnt- β -catenin signaling is enhanced after development in the adult cerebellum of SCA1 mice in an age-dependent manner, with the highest elevation occurring prior to end-stage PC degeneration (26–28).

To determine the specific cell types in which Wnt signaling is activated in SCA1, we utilized a transgenic reporter mouse (TCF/Lef:H2B-GFP) for the Wnt- β -catenin signaling pathway that uses a minimal promoter containing six TCF binding sites to express a H2B-GFP fusion protein upon canonical Wnt activation (Fig. 1*C* and *D*) (29). We crossed SCA1 KI mice with TCF/Lef:H2B-GFP mice and examined reporter activity in the cerebellum at 19 wk of age (Fig. 1*E* and *F*), a timepoint in which substantial gene-expression changes have been reported (30), and at which we observed elevated levels of Wnt- β -catenin target genes *Ccnd1* and *c-Myc* in SCA1 KI mice (Fig. 1*B*). WT reporter animals showed a baseline level of Wnt

signaling reporter activity in multiple cell types in adult cerebellum, including PCs (as indicated by the PC marker Calbindin, Calb1), as well as surrounding cell types in the granule cell layer (GCL) and molecular layer (ML) (Fig. 1*D* and *E*), supporting previous studies demonstrating that Wnt signaling persists into adulthood (9, 24, 25). SCA1 KI reporter mice exhibited an increased average GFP intensity (Fig. 1*F* and *G*) and increased proportion of PCs with higher intensity of Wnt- β -catenin signaling reporter activity in the cerebellum (Fig. 1*F* and *H*). Additionally, increase in reporter fluorescence was observed in other surrounding cell types in the ML, PC layer (PCL), and granular cell layer of the SCA1 KI cerebellum relative to WT reporter animals (Fig. 1*E* and *F*). Collectively, these results demonstrate that expression of polyQ-expanded ataxin-1 in the cerebellum increases canonical Wnt signaling activity in multiple different cerebellar cell types during SCA1 disease progression.

Ataxin-1 Positively Regulates Wnt- β -Catenin Signaling in a polyQ-Dependent Manner.

To determine the mechanism through which polyQ-expanded ataxin-1 affects the transcriptional output of Wnt- β -catenin signaling (Fig. 2*A*), we utilized an established β -catenin-responsive luciferase reporter, superTOPFlash (31) (Fig. 2*B*), which is activated by diverse upstream activators, including Wnt ligands, Dishevelled, LiCl (inhibitor of GSK3 β , a negative regulator of Wnt- β -catenin signaling), and β -catenin (Fig. 2*A*). Transfection of polyQ-expanded ataxin-1 strongly enhanced superTOPFlash activity in HeLa cells treated with Wnt3A conditioned media (Fig. 2*C*), confirming our in vivo finding that polyQ-expanded ataxin-1 is able to enhance Wnt- β -catenin signaling activity. To identify at which levels ataxin-1 modulates the Wnt- β -catenin signaling pathway, we performed similar luciferase reporter assays using Wnt- β -catenin signaling activators at different stages of the Wnt- β -catenin signaling cascade, including Dishevelled-3 transfection, LiCl treatment, and β -catenin transfection (Fig. 2*D–F*). We observed that in the absence of active Wnt signaling, ataxin-1 alone did not alter superTOPFlash activation. However, in all cases in which Wnt signaling was active, ataxin-1 could further enhance the level of superTOPFlash activation (Fig. 2*C–F*), suggesting that polyQ-expanded ataxin-1 likely operates in parallel with or downstream of β -catenin to enhance transcription of Wnt- β -catenin target genes in SCA1.

Transcriptional regulation of target genes in the canonical Wnt signaling pathway occurs via the coordination of β -catenin with several transcription factors following its translocation to the nucleus (32). To further elucidate how ataxin-1 regulates Wnt- β -catenin signaling, we performed coaffinity purification experiments to determine whether ataxin-1 physically interacts with the various transcription factors involved in canonical Wnt signaling, including β -catenin and TCF/LEF family members. Although canonical Wnt signaling requires β -catenin as a coactivator of transcription, no physical interaction between ataxin-1 and β -catenin was observed (Fig. 2*G*). However, a physical interaction between ataxin-1 and TCF/LEF family members LEF1 (HUGO name LEF1), TCF1 (HUGO name TCF7), TCF3 (HUGO name TCF7L1), and TCF4 (HUGO name TCF7L2) was observed (Fig. 2*H–K*). Interestingly, the interaction between ataxin-1 and Lef1 increased in a polyQ-dependent manner (Fig. 2*H*), providing a potential molecular mechanism for cell-autonomous ataxin-1-mediated Wnt- β -catenin signaling activation in SCA1. Overall, these data demonstrate that mutant ataxin-1 can physically interact with multiple effectors of Wnt- β -catenin target gene transcription and, in the presence of β -catenin, increase expression of downstream genes.

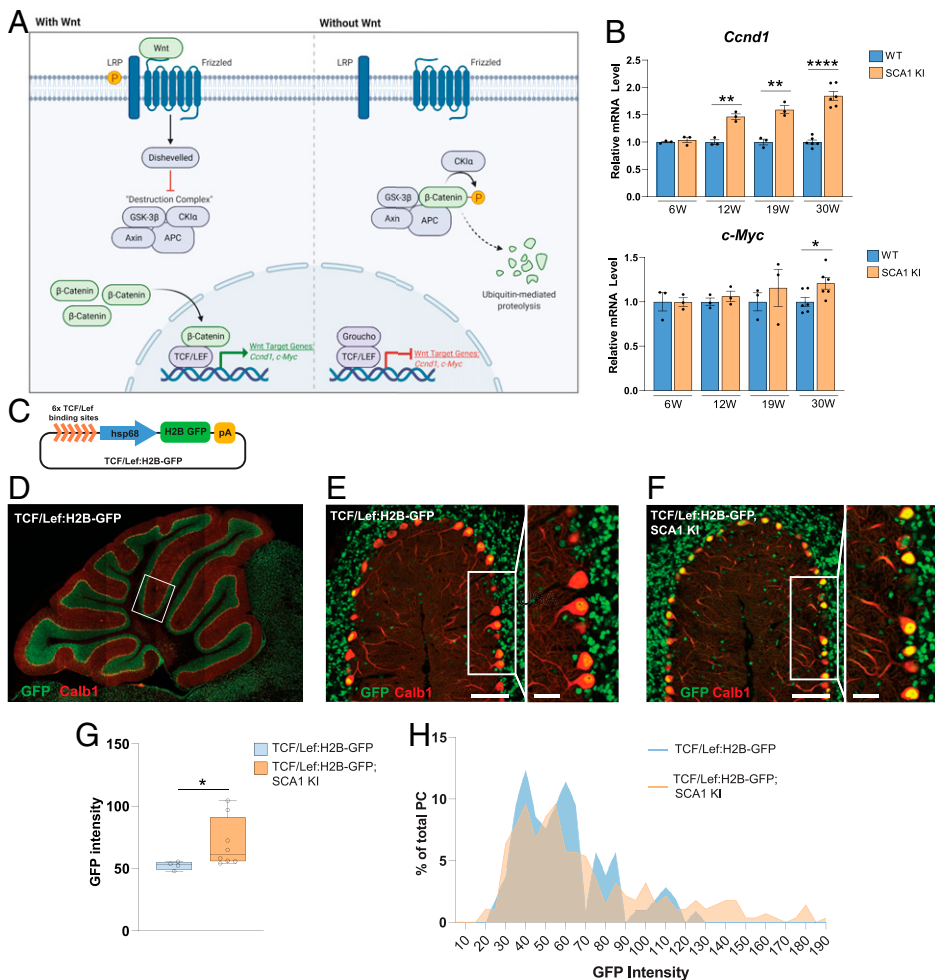


Fig. 1. Enhanced activation of Wnt- β -catenin signaling in the SCA1 KI mouse cerebellum. (A) Overview of Wnt- β -catenin signaling pathway. In the presence of Wnt ligands, β -catenin accumulates and translocates to the nucleus, where it binds with TCF family transcription factors to activate Wnt-responsive genes, including *Cnd1* and *c-Myc*. In the absence of Wnt ligands, β -catenin is degraded by a destruction complex. (B) RT-qPCR of Wnt- β -catenin target gene expression in SCA1 KI mouse cerebellum at 6, 12, 19, and 30 wk, normalized to WT littermate controls (6, 12, and 19 wk, $n = 3$ animals per genotype; 30 wk, $n = 6$ per genotype). (C) Schematics of Wnt- β -catenin signaling reporter (TCF/Lef:H2B-GFP). (D) Representative image of Wnt- β -catenin signaling reporter (TCF/Lef:H2B-GFP) cerebellum, stained with GFP (Wnt- β -catenin signaling activity) and Calbindin (Calb1, PC). (E and F) Representative images of 19 wk TCF/Lef:H2B-GFP (E) and TCF/Lef:H2B-GFP; SCA1 KI (F) mouse cerebellar lobule 5, stained with GFP and Calb1. (Scale bars, 100 μ m; *Inset*, 25 μ m.) (G and H) Quantification of intensity of Wnt- β -catenin signaling activity in PCs, as average GFP intensity in Calb1⁺ cells, with points representing image means (G) and as percentage of total PCs counted binned by GFP intensity (H) (TCF/Lef:H2B-GFP; SCA1 KI, $n = 2$; TCF/Lef:H2B-GFP, $n = 1$). * $P < 0.05$, ** $P < 0.01$, **** $P < 0.0001$, by Student's *t* test.

The pathogenicity of ataxin-1 is dependent on several key features and domains of the protein, including polyQ expansion, serine 776-phosphorylation, and its nuclear localization signal (33, 34). Therefore, we next investigated the involvement of these various features on Wnt induction by ataxin-1. First, longer ataxin-1 polyQ tract length resulted in increased superTOPFlash activation (Fig. 2*F*). Additionally, polyQ-expanded ataxin-1 carrying mutations of a key phosphorylation site (S776A) or nuclear localization signal (K772T) abrogated the activation of Wnt- β -catenin signaling by ataxin-1 (Fig. 2*L*). Because polyQ expansion, phosphorylation at S776, and the ability to localize to the nucleus are crucial for ataxin-1 pathogenicity, and modulating any of these properties mitigated the effect of ataxin-1 on Wnt- β -catenin signaling activation, these data reveal a mechanism through which pathogenic forms of ataxin-1 may contribute to transcriptional dysregulation in SCA1.

PC-Specific Expression of polyQ-Expanded Ataxin-1 Is Sufficient to Induce Cerebellar Wnt- β -Catenin Hyperactivation.

Next, to determine whether polyQ-expanded ataxin-1 can activate Wnt- β -catenin signaling through cell-autonomous mechanisms in PCs in vivo, we utilized a PC-specific transgenic mouse model of SCA1 in which polyQ-expanded ataxin-1 with 63 glutamine repeats was overexpressed in PCs (SCA1 Tg [63Q]), which was originated due to a germline contraction event from SCA1 Tg [82Q] line (35). Similar to SCA1 KI mice, transcript levels of Wnt target genes *Cnd1* and *c-Myc* were elevated in the cerebellum of SCA1 Tg [63Q] mice in an age-dependent manner compared to WT controls (Fig. 3*A*).

Interestingly, protein levels of active β -catenin, but not mRNA levels of *Ctnnb1*, were also elevated in the cerebellum of 30-wk SCA1 Tg [63Q] mice (Fig. 3*B–D*), suggesting posttranscriptional regulation of β -catenin levels by ataxin-1. Furthermore, we measured significant increases in GFP intensity, corresponding to Wnt- β -catenin signaling reporter activity, in PCs of 12-wk SCA1 Tg [63Q] mice crossed with TCF/Lef:H2B-GFP reporter mice, compared to control mice (Fig. 3*E–H*). Surprisingly, we found that the increased activity of Wnt- β -catenin signaling reporter was not only limited cell autonomously within the PCs of SCA1 Tg [63Q] cerebellum, but also noncell autonomously in other surrounding cell types in the PCL, as well as molecular and GCL (Fig. 3*E* and *F* and *SI Appendix*, Fig. S3). Finally, we found that expression of certain secreted Wnt ligands was elevated at 30 wk in SCA1 Tg [82Q] mice (*SI Appendix*, Fig. S4), which could contribute to the observed noncell-autonomous activation of Wnt signaling in surrounding cerebellar cell types. These data demonstrate that overexpression of polyQ-expanded ataxin-1 exclusively in PCs leads to enhanced activation of Wnt- β -catenin signaling cell autonomously in PCs, as well as surrounding cell types of the SCA1 cerebellum through indirect, noncell-autonomous mechanisms.

Genetic Manipulation of Canonical Wnt Signaling in PCs Has Minimal Impact on Cerebellar Health and PC Survival.

To determine whether enhanced Wnt- β -catenin signaling in PCs of SCA1 animals directly leads to neurodegeneration or is secondary to disease progression, we utilized multiple genetic approaches to conditionally suppress or activate Wnt- β -catenin signaling in a

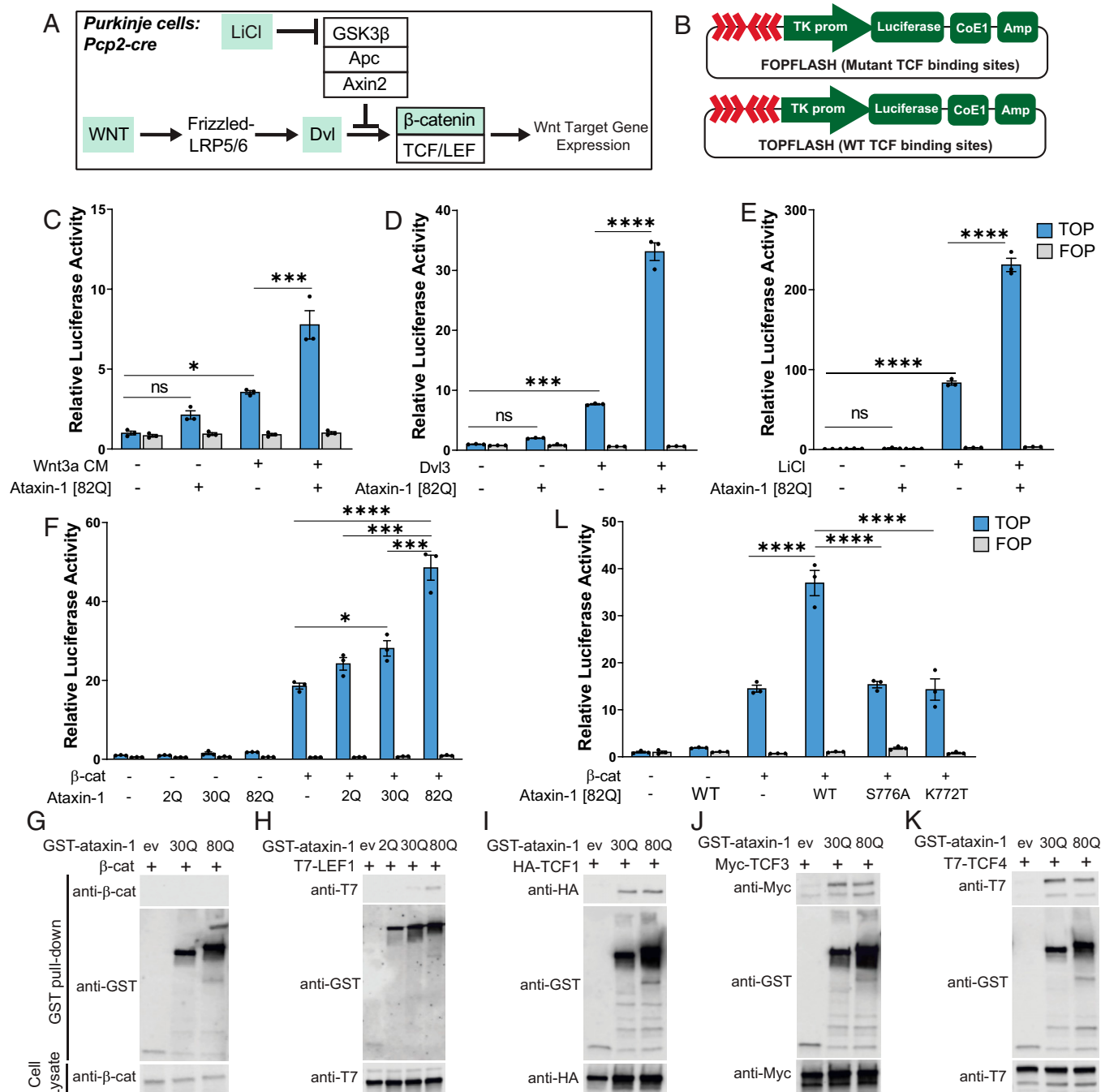


Fig. 2. Ataxin-1 activates Wnt- β -catenin signaling transcription in HeLa cells by binding to TCF family transcription factors. (A) Wnt- β -catenin signaling cascade schematic, with components of the pathway targeted in luciferase assay (C-F, and L) highlighted in green. (B) Schematic of TOPFlash, a β -catenin-responsive luciferase reporter, and FOPFlash, negative control, constructs, in which TCF binding sites trigger luciferase activity. (C-F), Quantification of luciferase activity (TOPFlash) upon cotransfection of HeLa cells with ataxin-1 [82Q] with Wnt- β -catenin signaling activators, including (C) Wnt3A- conditioned media (Wnt3a CM), (D) Dishevelled 3 (Dvl3), (E) LiCl treatment, an inhibitor of GSK3 β (negative regulator of Wnt signaling), and (F) β -catenin (β -cat) ($n = 3$ per treatment group). (G-K) Coaffinity purification assays of polyQ-expanded ataxin-1 of 30Q and 82Q length and TCF/ β -catenin transcription factors in HeLa cells, including (G) β -catenin, (H) LEF1, (I) TCF1, (J) TCF3, (K) TCF4. Upper panel shows expression of TCF/ β -catenin transcription factors and GST-ataxin-1 after affinity purification on glutathione-sepharose 4B beads. Lower panel shows total cell lysate. Ev, GST-empty vector. (L) PolyQ-expanded ataxin-1 enhances Wnt- β -catenin signaling while nonpathogenic forms of ataxin-1 do not in luciferase assay. S776A is phosphorylation-defective, K772T is nuclear localization-defective ($n = 3$ per treatment group). * $P < 0.05$, *** $P < 0.001$, **** $P < 0.0001$; ns, nonsignificant, by one-way ANOVA with Tukey's post hoc analysis.

cell-type-specific manner in WT and SCA1 mice (Figs. 4 and 5). We first assessed whether inhibition of Wnt- β -catenin signaling in PCs was able to rescue pathological or behavioral deficits in SCA1 through conditional deletion of *Ctmb1*, the gene encoding β -catenin, specifically in PCs (*Ctmb1* PC conditional knockout [cKO]; *Ctmb1*^{fl/fl}; *Pcp2-cre* mice) of both WT and SCA1 Tg [63Q] animals (Fig. 4A). Immunostaining confirmed successful removal of β -catenin in PCs of *Ctmb1* PC cKO mice, with

surrounding cells still maintaining β -catenin expression (Fig. 4B). Decreased, but not fully absent, levels of β -catenin protein were also confirmed in whole cerebellar extracts of *Ctmb1* PC cKO mice (Fig. 4C). Silencing Wnt- β -catenin signaling in PCs on a WT background did not significantly impact PC health during adulthood (Fig. 4 and SI Appendix, Fig. S5). As expected, ML thickness was reduced in SCA1 Tg [63Q] mice; however, this was not rescued by inhibition of Wnt- β -catenin signaling in

Ctmb1 PC cKO; SCA1 Tg [63Q] mice at 12, 20, or 30 wk compared to littermate controls (Fig. 4 *D* and *E*). Additionally, there were no significant changes in climbing fiber innervation between *Ctmb1* PC cKO; SCA1 Tg [63Q] and SCA1 Tg [63Q] mice at 12 or 20 wk (Fig. 4 *F* and *G*).

To confirm that these results were not due to the reduced polyQ length or background, we also analyzed ML thickness and climbing fiber innervation in an independent cohort of SCA1 transgenic animals overexpressing polyQ-expanded ataxin-1 with 82 repeats in PCs (SCA1 Tg [82Q]) (35). Similar to SCA1 Tg [63Q] mice, conditional deletion of *Ctmb1* in PCs of SCA1 Tg [82Q] animals did not rescue ML thickness in mice analyzed at 21 wk of age (*SI Appendix*, Fig. S5). Furthermore, silencing of Wnt- β -catenin signaling in PCs was not sufficient to decrease astrogliosis and microgliosis in SCA1 Tg [63Q] mice at 20 wk, as shown by *Gfap* and *Iba1* staining of astrocytes (AS) and microglia, respectively (Fig. 4 *H–K*). Finally, silencing Wnt- β -catenin signaling in PCs in SCA1 Tg [63Q] mice did not significantly affect motor performance, as assessed by accelerating rotarod, at 10 or 20 wk (*SI Appendix*, Fig. S6). These data demonstrate that inhibition of Wnt- β -catenin signaling in PCs specifically was not sufficient to prevent pathological and behavioral deficits observed in transgenic SCA1 mice.

We next sought to determine whether activation of Wnt- β -catenin signaling in PCs of WT mice alone was sufficient to induce SCA1-like phenotypes. To activate Wnt- β -catenin signaling in PCs, we generated *Apc* PC cKO (*Apc*^{fl/fl}; *Pcp2-cre*) mice in which the *Apc* gene, encoding a key component of the inhibitory destruction complex, was specifically deleted in PCs (Fig. 5*A*). We confirmed elevated β -catenin levels in the cerebellum of *Apc* PC cKO mice by immunostaining (Fig. 5*B*). We observed no significant changes in PC number (Fig. 5 *C* and *D*), molecular-layer thickness (Fig. 5 *E* and *F*), or climbing fiber innervation (Fig. 5 *G* and *H*) in 1-y-old *Apc* PC cKO mice compared to controls, demonstrating that activating Wnt- β -catenin signaling specifically in PCs alone is not sufficient to induce SCA1-like pathology. Additionally, activating Wnt- β -catenin signaling in PCs was not sufficient to induce SCA1-like behavioral deficits as assessed by accelerating rotarod, dowel rod, and wire hang (*SI Appendix*, Fig. S7). Together, these data suggest that elevated Wnt- β -catenin signaling in PCs observed in SCA1 does not have a profound impact on cerebellar health or disease progression.

Activation of Wnt- β -Catenin Signaling in BG Induces BG Mislocalization and Gliosis. As described earlier, we observed enhanced Wnt- β -catenin signaling not only in PCs, but in multiple cerebellar cell types in SCA1 KI and SCA1 Tg [63Q] mice (Figs. 1 *D–H* and 3 *E–H*). Because enhanced Wnt- β -catenin signaling in PCs alone was not sufficient to drive SCA1-like phenotypes (Fig. 5 and *SI Appendix*, Fig. S7), and genetically reducing Wnt signaling in PCs was not able to rescue SCA1 phenotypes (Fig. 4 and *SI Appendix*, Figs. S5 and S6), we next investigated the impact of elevated Wnt- β -catenin signaling in other cell types of the cerebellum. We were particularly interested in understanding the impact of Wnt- β -catenin signaling in BG, a specialized unipolar AS population exclusive to the cerebellum, for several reasons. First, BG closely associate with PCs and aid in PC synapse function and maintenance in adulthood through glutamate recycling and synaptic finetuning (36, 37). Second, BG-specific expression of polyQ-expanded ataxin-7, the disease-causing protein for SCA7, impairs glutamate transport via the reduction of GLAST, which is associated with noncell-autonomous PC loss (38). Interestingly, BG in a SCA1 mouse model similarly display

a reduction of GLAST (39), suggesting dysfunction of BG may contribute to eventual PC loss seen at late stages in SCA1. Finally, previous studies have shown that Wnt- β -catenin signaling activation in BG through *Apc* deletion is sufficient to cause neuronal loss in adult mice and cerebellar degeneration in a noncell-autonomous manner (22).

First, to confirm that polyQ-expanded mutant ataxin-1 expression in PCs can lead to noncell-autonomous Wnt- β -catenin signaling activation in other cell types, we analyzed Wnt reporter activity in BG of SCA1 Tg [63Q] reporter animals at 12 wk of age (Fig. 6 *A–D*). As was the case with PCs, Wnt reporter activity was significantly increased in Sox9⁺ BG in the SCA1 Tg [63Q] mouse cerebellum (Fig. 6 *A–D*). This confirmed that, in addition to cell-autonomous effects, expression of polyQ-expanded ataxin-1 in PCs leads to the enhanced activation of Wnt- β -catenin signaling in local cell types of the SCA1 cerebellum through indirect mechanisms.

We next examined the impact of enhanced Wnt- β -catenin signaling activation in BG. Activation of Wnt- β -catenin signaling in AS and BG populations through conditional deletion of *Apc* in *Gfap*⁺ cells (*Apc* AS cKO; *Apc*^{fl/fl}; *mGfap-cre*) (*SI Appendix*, Fig. S8*A*) caused a significant reduction in body weight compared to controls (*SI Appendix*, Fig. S8*B*), and was sufficient to increase β -catenin levels and induce severe astrogliosis (*SI Appendix*, Fig. S8 *C* and *D*), similar to what is observed in SCA1 mice (40). We also observed a significant decrease in GLAST (*Eaat1*) expression (39) (*SI Appendix*, Fig. S8 *C* and *E*). Furthermore, BG cell bodies were aberrantly mislocalized from the PCL to the ML in 4-wk-old *Apc* AS cKO mice (*SI Appendix*, Fig. S8 *F–I*), consistent with previous studies in which Wnt- β -catenin signaling was activated in BG (22). Due to this severe weight loss, we had to humanely kill *Apc* AS cKO mice around 4 wk, and therefore could not perform behavioral analyses.

Because Wnt- β -catenin signaling is activated in BG of SCA1 mice (Fig. 6 *A–D*) and genetic activation of Wnt- β -catenin signaling in BG is sufficient to induce BG mislocalization during development (*SI Appendix*, Fig. S8 *F–I*) (22), we next wanted to determine whether similar cellular phenotypes occurred in SCA1 mice, in which Wnt- β -catenin activation occurs in BG weeks after the cerebellar cytoarchitecture is established. To this end, we performed immunohistochemical staining for PCs (*Calb1*⁺ cells) and BG (*Sox9*⁺ cells) and quantified the number of BG in the PCL and ML (Fig. 6 *E–J* and *SI Appendix*, Fig. S9). Under physiological conditions, the majority of BG are expected to closely localize to the cell bodies of PCs in the PCL as a monolayer, which was observed in WT animals (Fig. 6 *E–J*). Similar to the *Apc* AS cKO mice (*SI Appendix*, Fig. S8 *F–I*), we observed a significant increase in the number of heterotopic BG in the ML, as well as significant increases in the ratio of BG cells in the ML/PCL, in 20-wk-old SCA1 Tg [82Q] mice (Fig. 6 *E–G*) and 30-wk-old SCA1 KI mice (Fig. 6 *H–J*). Interestingly, no significant differences were detected at 12 wk in SCA1 KI mice (Fig. 6 *I* and *J*, *Upper*), suggesting BG mislocalization occurs in an age-dependent manner. Considering the important roles of BG in PC maintenance and synapse function (41–45) and that *Apc* deletion in BG alone has been shown to be sufficient to induce cerebellar degeneration and PC loss (22), these data suggest that noncell-autonomous activation of Wnt- β -catenin signaling in BG in SCA1 results in disrupted BG to PC interactions that may contribute to cerebellar circuit dysfunction and disease pathogenesis.

We next aimed to assess whether inhibition of Wnt- β -catenin signaling in AS populations, including BG, may exhibit protective effects toward neuronal health and SCA1 pathology. To investigate this question, we first utilized *in vitro* cell culture

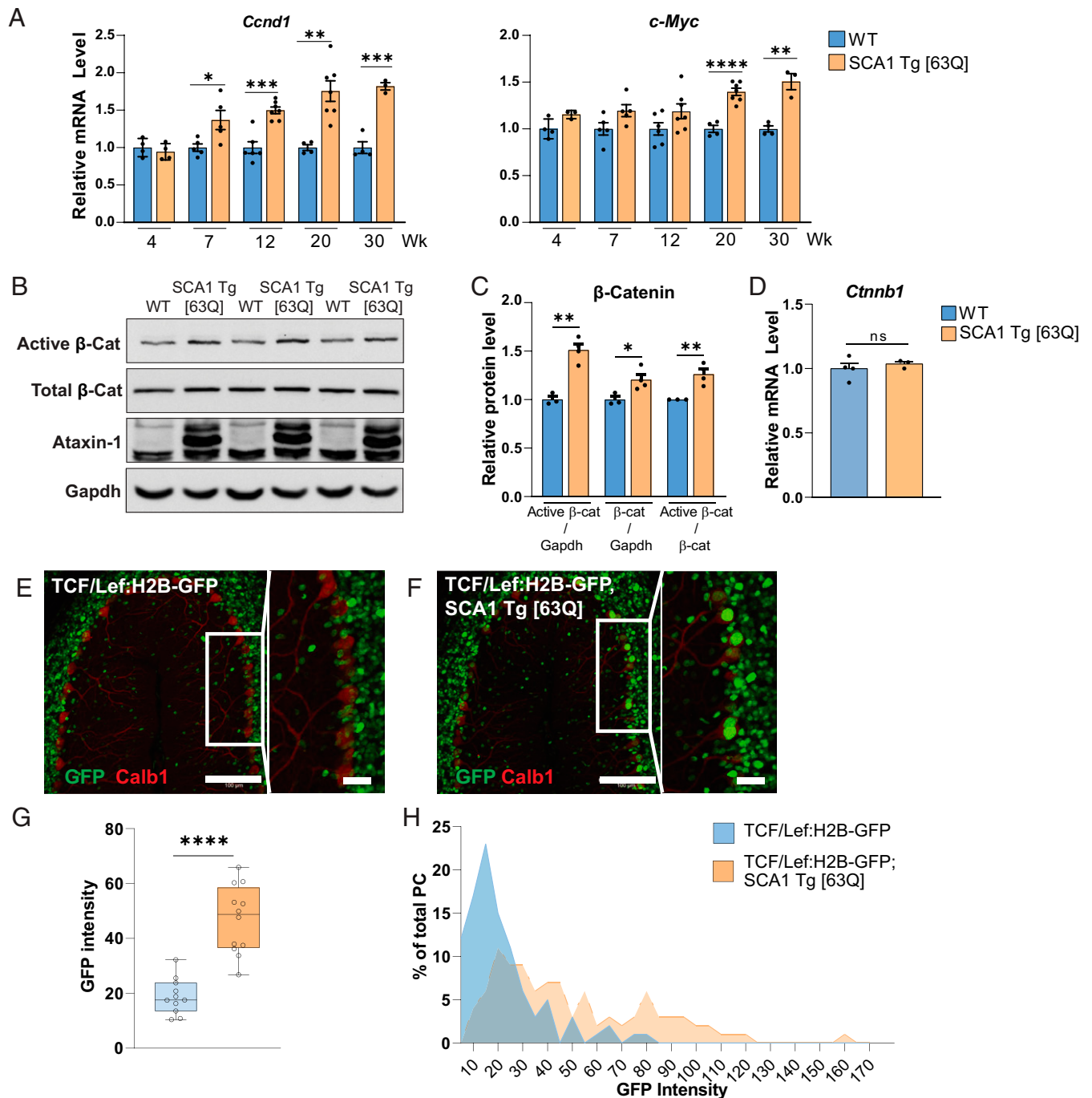


Fig. 3. Enhanced activation of Wnt-β-catenin signaling in the SCA1 Tg [63Q] mouse cerebellum. (A) RT-qPCR of Wnt-β-catenin target gene expression in SCA1 Tg [63Q] mouse cerebellum at 4, 7, 12, 20, and 30 wk, normalized to WT littermate controls ($n = 3$ to 7 animals per genotype). (B) Western blot images of β-catenin protein expression (total and active forms) and ataxin-1 protein expression in whole cerebellar extracts of WT and SCA1 Tg [63Q] mice at 30 wk. Gapdh was used as a loading control. (C) Quantification of total and active β-catenin protein expression levels from (B), normalized to Gapdh and WT expression levels (WT, $n = 3$; SCA1 Tg [63Q], $n = 4$). (D) RT-qPCR of *Ctnnb1* mRNA expression in SCA1 Tg [63Q] mouse cerebellum at 30 wk, normalized to WT littermate controls ($n = 3$ per genotype). (E and F) Representative images of 12-wk TCF/Lef:H2B-GFP (E) and SCA1 Tg [63Q]; TCF/Lef:H2B-GFP (F) mouse cerebellar lobule 5, stained with Calb1 and GFP. (Scale bars, 100 μm; *Inset*, 25 μm.) (G and H), Quantification of intensity of Wnt-β-catenin signaling activity in PCs, as average GFP intensity in Calb1⁺ cells, with points representing image means (G) and as percentage of total PCs counted binned by GFP intensity (H) (TCF/Lef:H2B-GFP; SCA1 Tg [63Q], $n = 4$; TCF/Lef:H2B-GFP, $n = 3$). * $P < 0.05$, ** $P < 0.01$, *** $P < 0.001$, **** $P < 0.0001$, by Student's *t* test.

methods in which we cultured Neuro-2a (N2A) cells with SCA1 AS-conditioned media (ACM) from clonal astrocytic C8S cells, which are derived from the mouse cerebellum and exhibit radial BG-like morphology (46) (SI Appendix, Fig. S10). Transfection of Flag-hATXN1 [82Q] in C8S cells (SI Appendix, Fig. S10B) was sufficient to enhance Wnt-β-catenin target gene expression in vitro (SI Appendix, Fig. S10 C–E). We found that silencing Wnt-β-catenin signaling in C8S cells by *Ctnnb1* siRNA

(SI Appendix, Fig. S10F) was sufficient to reduce expression of apoptotic marker cleaved caspase-3 (CC3) in N2A cells treated with SCA1 ACM, compared to control siRNA (SI Appendix, Fig. S10 G and H). These data suggest that in vitro, silencing Wnt-β-catenin signaling in AS alone is sufficient to rescue markers of neuronal pathology.

To investigate whether silencing Wnt-β-catenin signaling in AS and other diverse cell types is able to rescue SCA1

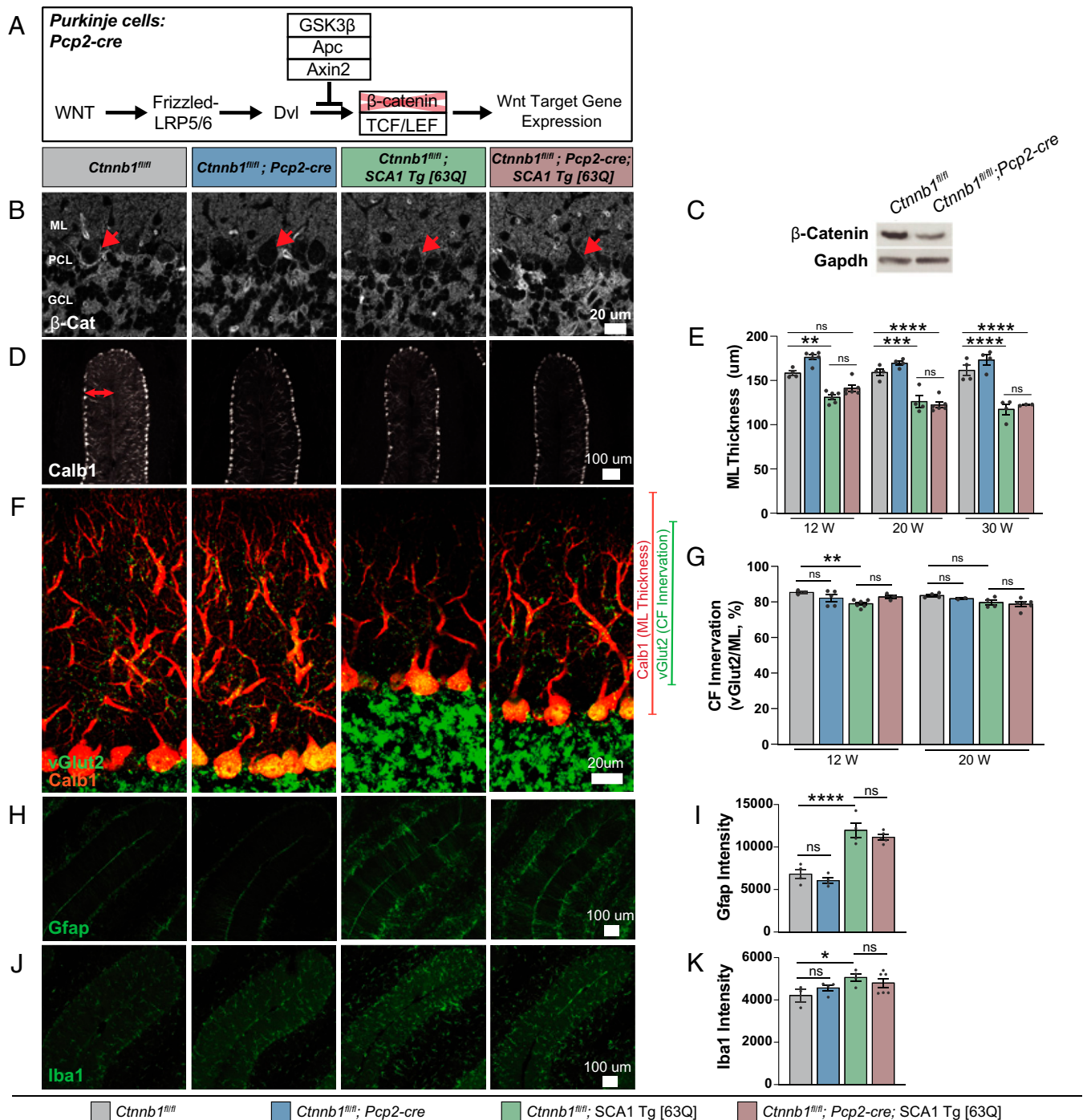


Fig. 4. Loss of Wnt- β -catenin signaling in PCs does not prevent SCA1 phenotypes in SCA1 Tg [63Q] mice. (A) Schematic of Wnt- β -catenin signaling silencing in PCs by *Ctnnb1* conditional deletion. (B) Immunohistochemistry showing loss of β -catenin in the PCs of *Ctnnb1* PC cKO (*Ctnnb1*^{fl/fl}; *Pcp2-cre*) mice, with arrows indicating PCs, scale bar 20 μ m. (C) Representative Western blot images of β -catenin protein expression in whole cerebellar extracts of control and *Ctnnb1* PC cKO mice, with Gapdh as loading control. (D and E) Representative images of Calb1 staining of 20 wk cerebellar lobule 5 in control and *Ctnnb1* PC cKO mice on WT and SCA1 Tg [63Q] backgrounds (D), to measure ML thickness quantified at 12, 20, and 30 wk (E), $n = 4, 4, 6, 6$ (12 wk), $n = 4, 4, 4, 3$ (30 wk), scale bar 100 μ m. (F and G) Representative images of vGlut2 and Calb1 staining of 20-wk cerebellar lobule 5 in control and *Ctnnb1* PC cKO mice on WT and SCA1 Tg [63Q] backgrounds (F), to quantify climbing fiber (CF) innervation (ratio of vGlut2/ML thickness) at 12 and 20 wk (G) $n = 4, 6, 6, 6$ (12 wk), $n = 4, 4, 4, 6$ (20 wk), scale bar 20 μ m. (H) Representative images of Gfap staining at 20 wk in control and *Ctnnb1* PC cKO mice, on WT and SCA1 Tg [63Q] backgrounds, quantified in (I) $n = 4, 4, 4, 5$, scale bar 100 μ m. (J) Representative images of Iba1 staining at 20 wk in control and *Ctnnb1* PC cKO mice, on WT and SCA1 Tg [63Q] backgrounds, quantified in (K), $n = 3, 4, 4, 6$, scale bar 100 μ m. * $P < 0.05$, ** $P < 0.01$, *** $P < 0.001$, **** $P < 0.0001$, ns, nonsignificant, by one-way ANOVA with Tukey's post hoc analysis.

pathology in vivo, we analyzed SCA1 Tg [82Q] mice in which β -catenin expression had been constitutively reduced by 50% in all cell types, including AS populations (*Ctnnb1* KO/+; SCA1 Tg [82Q]). We confirmed successful reduction of β -catenin protein expression in the heterozygous *Ctnnb1* KO/+ lines (SI Appendix, Fig. S11 A and B). As expected, we observed PC loss, ML thinning, and climbing fiber denervation in SCA1

Tg [82Q] mice at 30 wk (SI Appendix, Fig. S11 C–H). This SCA1 pathology was not rescued by a constitutive 50% knock-down of Wnt- β -catenin signaling (SI Appendix, Fig. S11 C–H).

Taken together, these in vitro and in vivo data suggest that activation of Wnt- β -catenin signaling in AS is sufficient to cause SCA1-like glial pathology (Fig. 6 and SI Appendix, Figs. S8 and S9), and that near complete silencing of Wnt- β -catenin

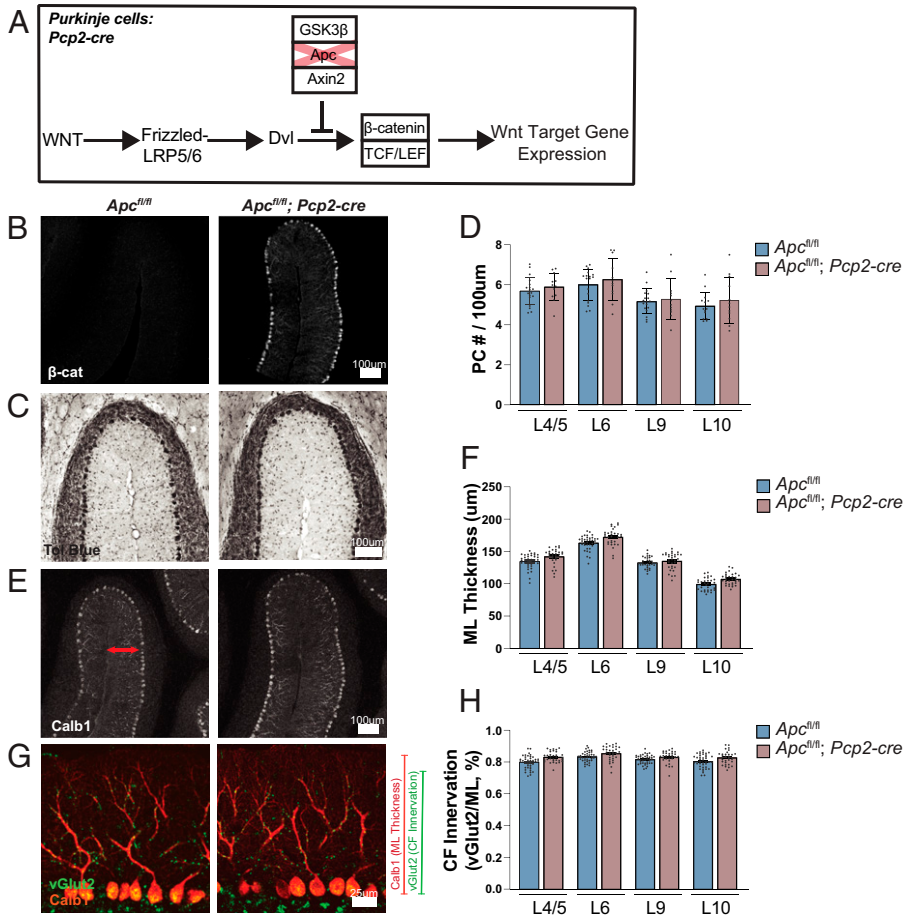


Fig. 5. Ectopic activation of Wnt- β -catenin signaling in PCs does not induce SCA1-like phenotypes. (A) Schematic of Wnt- β -catenin signaling activation in PCs by conditional *Apc* deletion. (B) Representative images of β -catenin staining in cerebellar lobule 5, showing up-regulation of β -catenin intensity in *Apc* PC cKO (*Apc^{fl/fl}; Pcp2-cre*) mice compared to controls (*Apc^{fl/fl}*). (C–H) Representative images of Toluidine blue (C), Calb1 (E), and Calb1 and vGlut2 (G) staining of cerebellar lobule 5 in 1-y-old control and *Apc* PC cKO mice, quantified in D, F, and H). (Scale bars, 100 μ m in C and E, and 25 μ m in G.) (D, F, and H) Quantifications of PC number per 100 μ m; (D) ML thickness in micrometers (F) and climbing fiber innervation, as ratio of vGlut2/ML thickness (H) in lobules 4/5, 6, 9 and 10 of 1-y-old *Apc* PC cKO and control mice, (*Apc* PC cKO $n = 5$, control $n = 4$). Points in bar plots indicate measurements per image.

signaling in SCA1 AS has neuroprotective effects in vitro (SI Appendix, Fig. S10). However, 50% reduction of Wnt- β -catenin signaling in vivo was not sufficient to rescue SCA1 pathology in transgenic SCA1 mice (SI Appendix, Fig. S11).

Discussion

The cerebellar cortex circuit is comprised of multiple cell types that intricately interact to produce a coordinated output to the deep cerebellar nuclei via PCs, a population of neurons unique to the cerebellum that undergoes degeneration in many SCAs (2, 47). How individual cell types contribute to cerebellar dysfunction and PC degeneration in SCAs remains an outstanding question. In this study, we found that ataxin-1, the protein mutated in SCA1, positively regulates Wnt- β -catenin signaling in a polyQ-dependent manner and that canonical Wnt- β -catenin signaling is activated in several SCA1 mouse models in an age-dependent manner in multiple cerebellar cell types, including PCs and BG. To determine the impact of this increased signaling activity in different cell types, we used cell-type-specific mouse models to activate or inhibit Wnt- β -catenin signaling in PCs and BG and found that the impact of Wnt- β -catenin signaling in the adult cerebellum was greater in BG rather than PCs, highlighting the importance of glia in SCA1 pathology and disease progression. We show that in vitro silencing of Wnt- β -catenin signaling in AS is able to reduce apoptotic marker expression in N2A cells treated with ACM. However, constitutive 50% reduction Wnt- β -catenin signaling in vivo is not able to rescue SCA1 pathology. This could suggest that complete silencing of Wnt- β -catenin signaling is needed to rescue pathology, or that continued activation

of other signaling pathways in SCA1 is sufficient to still drive SCA1 pathology, or both. Future studies targeting multiple disease-causing pathways, or fine-tuning the degree of Wnt- β -catenin signaling silencing in glial cell types, would be beneficial (Fig. 7).

We also provide a mechanism through which ataxin-1 positively regulates Wnt- β -catenin signaling activity. We found that ataxin-1 enhances Wnt- β -catenin signaling activity at multiple levels of the pathway, and that this is dependent on the presence of pathogenic features of ataxin-1, including polyQ expansion, serine 776-phosphorylation, and nuclear localization. This provides a cell-autonomous mechanism for the enhanced activation of Wnt- β -catenin signaling in SCA1 PCs and presumably in other cell types expressing ataxin-1, potentially through direct interaction with TCF/LEF family members. Our studies also provide a potential noncell-autonomous mechanism in which elevated expression of Wnt ligands in any given cell type could activate Wnt- β -catenin signaling in surrounding cell types. Enhanced Wnt ligand secretion may also explain the dysregulation of genes associated with planar cell polarity (PCP) signaling, a noncanonical Wnt signaling pathway, observed in SCA1 in previous studies (8). Although expression of mutant ataxin-1 in the cerebellum is primarily limited to PCs in the transgenic animal models used here, the cellular source of enhanced Wnt ligand production is unclear. While it is possible that PCs expressing polyQ-expanded ataxin-1 may cell autonomously increase Wnt ligand production, it is also possible that PC dysfunction may noncell autonomously stimulate other local cell types of the cerebellar cortex to increase production of Wnt ligands. Furthermore, although increased secretion of Wnt ligands can contribute to local

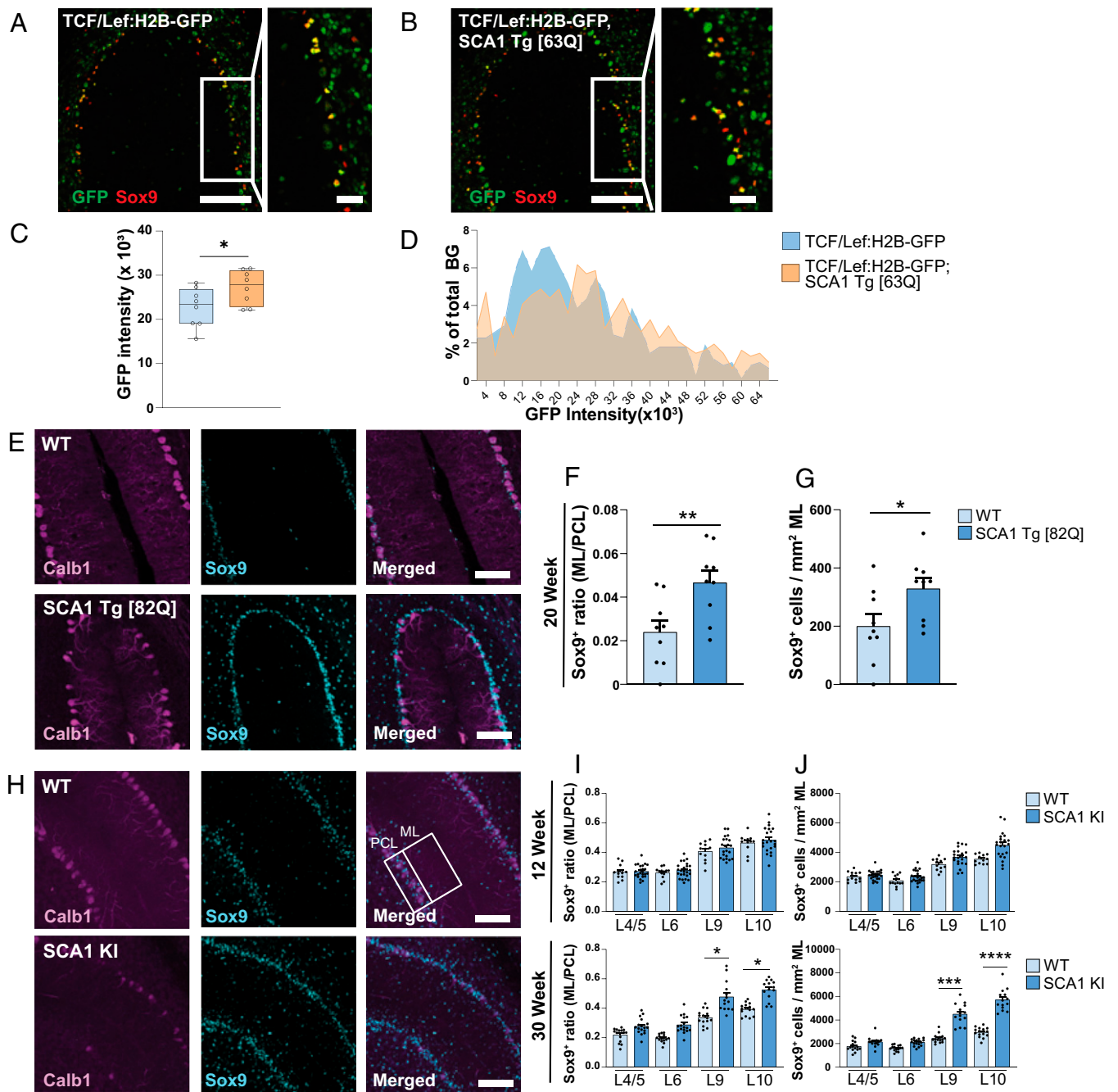


Fig. 6. Noncell-autonomous Wnt- β -catenin signaling activation in BG in SCA1 mice and BG mislocalization phenotypes in SCA1. (A and B) Representative images of 12-wk TCF/Lef:H2B-GFP (A) and TCF/Lef:H2B-GFP; SCA1 Tg [63Q] (B) mouse cerebellar lobule 5, stained with GFP and Sox9. (Scale bars, 100 μ m; *Inset*, 25 μ m.) (C and D) Quantification of intensity of Wnt- β -catenin signaling activity in BG, as average GFP intensity in Sox9⁺ cells, with points representing image means (C) and as percentage of total BG counted binned by GFP intensity (D). (E) Representative images of Calb1⁺ PCs and Sox9⁺ BG in 20-wk SCA1 Tg [82Q] and WT cerebellar lobule 4/5. (Scale bars, 100 μ m.) (F and G) Quantification of ratio of Sox9⁺ BG in ML/PCL (F), and number of Sox9⁺ BG in ML (G) in 20-wk cerebellar lobules L4/5 SCA1 Tg [82Q] and WT controls ($n = 3$ per genotype). (H) Representative images of immunostaining for Calb1⁺ PCs, and Sox9⁺ BG in 30-wk WT and SCA1 KI cerebellar lobule 9. (Scale bars, 100 μ m.) (I and J) Quantification of ratio of Sox9⁺ BG in ML/PCL (I), and number of Sox9⁺ BG in ML (J) in 12 wk (*Upper*) and 30 wk (*Lower*) cerebellar lobules L4/5, L6, L9, and L10 for SCA1 KI and WT controls (WT 12-wk $n = 3$, WT 30-wk $n = 3$, SCA1 KI 12-wk $n = 4$, SCA1 KI 30-wk $n = 5$). * $P < 0.05$, ** $P < 0.01$, *** $P < 0.001$, **** $P < 0.0001$, by Student's *t* test (C, F, and G), and by one-way ANOVA with Tukey's post hoc analysis (I and J). For F, G, I, and J, points indicate measurements per image.

Wnt activation in adjacent cell types, it is possible that noncell-autonomous Wnt activity can also be influenced by altered inflammatory states of the various glial populations of the cerebellum, in which changes in intracellular signaling pathways that reciprocally regulate Wnt- β -catenin signaling, such as NF- κ B, have been reported (40, 48, 49). However, the degree to which activation of BG contributes to enhanced Wnt activity in SCA1 independent of extracellular Wnt ligands, remains to be determined.

We observed enhanced Wnt- β -catenin signaling in additional cell types, besides PCs and BG, in our SCA1 mouse models in an age-dependent manner compared to controls. Future studies to investigate which other cell types exhibit enhanced Wnt- β -catenin signaling in SCA1 mice are needed. Furthermore, whether this activation of Wnt- β -catenin signaling in those cell types is protective, toxic, compensatory, or secondary to SCA1 disease progression requires further investigation. Interestingly, Wnt signaling has been implicated in other neurodegenerative diseases,

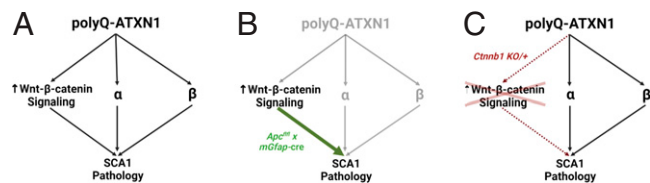


Fig. 7. Schematic summary of proposed model. (A) Wnt- β -catenin signaling, along with other pathways (represented as α and β), is progressively altered in SCA1 by ataxin-1 in a polyQ-dependent manner. (B) Activating Wnt- β -catenin signaling alone in AS populations is sufficient to induce SCA1-like glial pathology. (C) Fifty-percent constitutive reduction of Wnt- β -catenin signaling alone in SCA1 background is not sufficient to rescue SCA1 pathology in vivo, underscoring the remaining contribution of other pathways toward SCA1 pathogenesis.

including Alzheimer's disease (50–54), amyotrophic lateral sclerosis (55, 56), and Huntington's disease (57), and a rare form of ataxia (58). Previous studies of the impact of Wnt- β -catenin signaling in Alzheimer's disease suggest enhanced signaling may be protective against the toxicity of A β peptides, including synapse loss (59). In contrast, enhanced β -catenin levels are thought to be toxic in Huntington's disease and a rare form of ataxia (57, 58). Studies in NEDAMSS, a rare neurodevelopmental form of ataxia, found inhibition of Wnt signaling in neurons and AS to be neuroprotective (58).

In addition to being implicated in neurodegeneration, the dysregulation of Wnt- β -catenin signaling in cancer and the role of this signaling pathway in cancer cell proliferation have also been well characterized (60, 61). Previous studies describe an association between ataxin-1 and cancer cell proliferation (62), which could potentially occur through Wnt- β -catenin signaling based on our data. Interestingly, there have also been studies indicating a lower incidence of cancer across polyQ expansion diseases, including SCAs and Huntington's disease (63, 64). Therefore, future studies to further investigate the relationship between the Wnt- β -catenin signaling and SCAs in cancer would be of interest. Our studies here in SCA1 suggest that activation of Wnt- β -catenin signaling impacts unique cell populations in the cerebellum differently, and highlight the importance of examining signaling pathways in the specific cellular contexts in which they may be affected. Our data indicate that while activation of Wnt- β -catenin in PCs does not significantly contribute to SCA1 phenotypes, activation of Wnt- β -catenin signaling in BG is detrimental and sufficient to cause gliosis and BG mislocalization in *Apc* AS cKO mice. The exact cellular mechanisms through which BG impact PC health and SCA1 pathology are still unclear. However, we observed reduced expression of GLAST (Eaat1) in *Apc* AS cKO mice, which may serve as a mechanism in which activation of Wnt- β -catenin signaling in AS impacts PC health, as previously shown in SCA1 mice (39). Overall, these findings underscore the complex cell-cell interactions underlying SCA1 pathogenesis and bring attention to the role of BG in PC survival and in SCA1 disease progression.

Materials and Methods

Animal Husbandry. All animal care procedures were approved by the Yale University Institutional Animal Care and Use Committee. Mice were kept in a 12-h light/dark cycle with standard chow and ad libitum access to water. A combination of males and females were used for all experiments. Three mouse models of SCA1 were utilized: an SCA1 KI (*Atn1*^{154Q/+}) (26) strain, which expresses mutant ataxin-1 with 154 glutamine repeats under its endogenous promoter; an SCA1 transgenic (SCA1 Tg [82Q]; *Pcp2-ATXN1*^{82Q/+}) (35) line, in which mutant ataxin-1 with 82 glutamine repeats is overexpressed under the PC-specific *Pcp2* promoter; and a SCA1 transgenic (SCA1 Tg [63Q]; *Pcp2-ATXN1*^{63Q/+}) line, in which the polyQ tract length was reduced to 63 glutamine

repeats due to a germline contraction event. These lines were crossed with a Wnt- β -catenin reporter line (TCF/Lef:H2B-GFP) (29), in which Wnt- β -catenin activity drives GFP expression in cells. Additionally, the SCA1 Tg [63Q] and SCA1 Tg [82Q] lines were crossed with *Cttnb1* PC cKO (*Cttnb1*^{fl/fl}; *Pcp2-cre*), *Apc* PC cKO (*Apc*^{fl/fl}; *Pcp2-cre*), and *Apc* AS cKO (*Apc*^{fl/fl}; *mGfap-cre*) lines, in which Wnt- β -catenin signaling is activated or inhibited in PC (under the PC-specific *Pcp2* promoter) or AS (under the AS-specific *mGfap* promoter) populations specifically. The SCA1 Tg [82Q] mice, on an FVB background, were crossed with heterozygous constitutive *Cttnb1* KO (*Cttnb1* KO/+) mice, on a C57BL/6J background, which were generated in house using *Cttnb1*^{fl/fl} strains. *Cttnb1*^{fl/fl} (Jackson Laboratory stock no. 004152), TCF/Lef:H2B-GFP (Jackson Laboratory stock no. 013752), *mGfap-cre* (Jackson Laboratory stock no. 012886), and *Apc*^{fl/fl} (EMMA mouse repository, stock no. EM:05566) strains were purchased commercially. SCA1 Tg [63Q] mice were originally maintained on a FVB background and back-crossed onto C57BL/6J for three generations before analyses. All other mice and littermates were maintained on a C57BL/6J background.

Cell Culture. C8S (ATCC, CRL-2535, Astrocyte type II clone) cells were plated at 2×10^5 cells per 12-well plate 24 h prior to transfection, maintained in a 37 °C, 5.5% CO₂ incubator. When 70 to 80% confluent, C8S cells were transfected with 1 μ g of Flag-hATXN1 [82Q] plasmid, Lipofectamine 3000 (Invitrogen, L3000015), P-3000 (Invitrogen, L3000015), and Opti-MEM. Following an 8-h transfection period, media was changed and C8S cells were transfected with 20 nM control siRNA (Dharmacon, ON-TARGETplus nontargeting control pool, D-001810-10-20) or *Cttnb1* siRNA (Dharmacon, ON-TARGETplus SMARTpool, L040628-00-0005), Lipofectamine 3000 (Invitrogen, L3000015), and Opti-MEM for 12 h. ACM was transferred to untreated N2A (ATCC, CCL-131) cells the following day. N2A cells had been plated at 2×10^5 cells per 12-well plate 24 h prior to addition of ACM and maintained in a 37 °C, 5.5% CO₂ incubator. C8S cells were subsequently collected and transferred into 500 μ L PBS and centrifuged for 3 min at 10,000 rpm. RNA was extracted from pelleted C8S cells using Qiagen RNeasy Mini Kit, following the manufacturer's instructions. N2A cells were cultured with ACM for 24 h, and subsequently collected and transferred into 500 μ L PBS and centrifuged for 3 min at 10,000 rpm. Protein was extracted from pelleted N2A cells and used for Western blot analysis.

Protein Extraction and Western Blot Analysis. Mouse cerebellar tissue was homogenized in Triple lysis buffer (0.5% Nonidet P-40, 0.5% Triton X-100, 0.1% SDS, 20 mM Tris-HCl [pH 8.0], 180 mM NaCl, 1 mM EDTA, and Roche complete protease inhibitor mixture and PhosStop protease inhibitors) by dounce homogenization on ice. N2A cells were lysed in RIPA buffer (1% Nonidet P-40, 0.1% SDS, 50 mM Tris-HCl [pH 8.0], 150 mM NaCl, 0.5% sodium deoxycholate, and Roche complete protease inhibitor mixture and PhosStop protease inhibitors). Samples were then sonicated to ensure breakdown of protein aggregates before rotation at 4 °C for 10 min and centrifugation for 10 min at 13,000 rpm at 4 °C. Total protein concentration of the supernatant was quantified using a BCA assay (ThermoFisher 23225) and equal protein amounts were boiled at 95 °C for 10 min prior to being run on a gel (Bio-Rad) at 120V. Proteins from gels were transferred for one hour at 100V at 4 °C onto 0.45- μ m nitrocellulose membranes. Membranes were washed with TBST (Tris-buffered saline, 0.1% Tween-20) three times for 10 min each, followed by 1 h of blocking in 5% nonfat dry milk in TBST at room temperature. Membranes were then incubated with primary antibody in 5% nonfat dry milk in TBST at 4 °C overnight. The following day, membranes were washed with TBST three times for 10 min each, followed by incubation in either sheep anti-mouse or donkey anti-rabbit IgG-conjugated with horseradish peroxidase (HRP) (Millipore Sigma, GENA931, GENA934; 1:4,000) in TBST at room temperature for 2 h. Membranes were then washed with TBST three times for 10 min and developed using SuperSignal West Pico Plus Chemiluminescent substrate (Pierce, Cat. 34580) and visualized using a KwikQuant Imager (Kindle Biosciences). Images were quantified using ImageJ. The following primary antibodies were used: Mouse anti-Gapdh (Sigma G8795; 1:10,000), mouse anti-Vinculin (Millipore v9264; 1:10,000), mouse anti- β -catenin (BD 610154; 1:20,000), mouse antiactive β -catenin (Millipore 06-665; 1:500), rabbit antiataxin-1 (11750; 1:1,000), mouse anti-T7 (Novagen 69522; 1:10,000), rabbit anti-HA (Abcam ab9110; 1:5,000), mouse anti-c-Myc (Sigma M5546 clone 9e10; 1:1,000), rabbit anti-CC3 (Cell Signaling 9661L; 1:500), and rabbit anti-GST (Sigma G7781; 1:3,000).

RNA Extraction and RT-qPCR. RNA was extracted from frozen mouse cerebellar tissue and C8S cell pellets using the Qiagen RNeasy Mini Kit, following the manufacturer's instructions. cDNA was synthesized using oligo-dT primers and iScript cDNA synthesis kit (Bio-Rad, 1708891). Reverse transcription-quantitative PCR (RT-qPCR) was performed using TaqMan probes with iTaq Universal Probe Supermix on a C1000 Thermal Cycler (Bio-Rad). The following TaqMan (Applied Biosystems) probes were used: *Gapdh* (4352661, Mm99999915_g1), *Actb* (4352933E, Mm00607939_s1), *Hprt* (4331182, Mm03024075_m1), *ATXN1* (4331182, Hs00165656_m1), *Ccnd1* (4331182, Mm00432359_m1), *Myc* (4331182, Mm00487804_m1), *Axin2* (4331182, Mm00443610_m1). Custom TaqMan array plates (ThermoFisher, 4413261) were used for the Wnt ligand screen, with the following TaqMan probes: *Actb* (Mm00607939_s1), *Gapdh* (Mm99999915_g1), *Hprt* (Mm00446968_m1), *Wnt2* (Mm00470018_m1), *Wnt2b* (Mm00437330_m1), *Wnt3* (Mm00437336_m1), *Wnt4* (Mm01194003_m1), *Wnt5a* (Mm00437347_m1), *Wnt6* (Mm00437353_m1), *Wnt7a* (Mm00437356_m1), *Wnt8b* (Mm00442108_g1), *Wnt10a* (Mm00437325_m1), *Wnt10b* (Mm00442104_m1), *Wnt11* (Mm00437327_g1). All samples were loaded in triplicate. Target gene expression was normalized to housekeeping genes (*Actb*, *Gapdh*, and *Hprt*) using Bio-Rad CFX manager software and plotted relative to mean expression of controls.

Immunofluorescence Staining. Mice were anesthetized prior to intracardial perfusion with phosphate buffered saline (PBS) and 4% paraformaldehyde (PFA). Brains were postfixed overnight in 4% PFA before incubation in 20% and 30% sucrose in PBS. Samples were frozen in OCT compound (VWR, 4538) and sliced into 30- μ m sections on a cryostat (Leica). Free-floating sections were washed in PBS and PBS with 0.1% Triton-X before incubation in 5% normal goat serum (Jackson Labs, 005-000-121) at room temperature. Upon usage, antigen retrieval with 10 mM citric acid for 30 min was used before wash and incubation in primary antibody. Primary antibody incubation was carried out at 4 °C overnight with the following antibodies: mouse anticalbindin-D-28K (Sigma, C9848; 1:1,000), rabbit anti-vGlut2 (Synaptic Systems, 135402; 1:500), rabbit anti- β -Catenin (Sigma, AV14001; 1:1,000), mouse anti- β -catenin (BD Transduction Laboratories, 610154; 1:1,000), chicken anti-Gfap (Abcam, ab4674; 1:1,000), rabbit anti-Iba1 (Wako, 019-19741; 1:500), rabbit anti-Sox9 (1:500), rabbit anti-Eat1 (Cell Signaling, D44E2; 1:500), and rabbit anti-GFP (Abcam, ab290; 1:4,000). Sections were washed in PBS with 0.1% Triton-X before incubation in secondary antibody (Invitrogen AlexaFluor; 1:500) then washed and mounted onto slides and coverslipped with Vectashield mounting media and DAPI (Vector Laboratories, H-1500). Fluorescent images were acquired on a Zeiss LSM800 or LSM880 confocal microscope, using the same microscope and settings across similar experiments. Between three and six brain sections were imaged and quantified for each mouse.

Fluorescent Image Quantification. ImageJ (NIH) was used for all image processing and quantification. For fluorescent intensity quantification, image z-stacks were flattened to maximum intensity z-projection, converted to 8-bit images, and thresholded using identical parameters across all images. ROI (region of interest) manager was used to measure equal areas across images. For GFP fluorescent intensity quantification in PCs or BG, calbindin (for PCs), or Sox9 (for BG) images were thresholded, and overlaid onto the GFP images. The mean gray intensity value was recorded. For quantification of number of GFP⁺ cells in the GCL, image z-stacks were flattened to maximum-intensity z-projection, converted to 8-bit images, and thresholded using equal parameters across all images. ROI manager was used to measure equal areas of the GCL. The watershed function was utilized to split clumped nuclei, and only GCL nuclei greater than 20 μ m² were counted. To measure the ML thickness, the lengths of the PC dendrites were measured at six locations in the image, from the tip of the PC soma until the end of the ML ~300 μ m from the tip of the specified cerebellar lobule. For calbindin intensity across the ML, a similar methodology was employed as previously described (26). Briefly, the z-stack was flattened in ImageJ using the average intensity z-projection, and the intensity per pixel plotted using plot profile. Three PCs ~300 μ m from the tip of the lobule per section were used for quantification, and the average intensity value for 1- μ m increments plotted for each animal. For assessing the innervation of inferior olive climbing fiber vGlut2 puncta along PC dendrites, a z-stack corresponding to a 5- μ m depth was flattened in ImageJ using the maximum-intensity z-projection. The length of vGlut2 innervation relative to the length of the ML was measured at three separate locations along the lobule, similar

to the methodology for assessing calbindin intensity. For assessing Sox9⁺ BG distribution, image z-stacks were flattened to maximum-intensity z-projection, converted to 8-bit images, and thresholded using equal parameters across all images. ROI manager was used to measure equal areas across images for the PC layer and ML. The watershed function was utilized to split clumped nuclei, and only BG with nuclei greater than 3 μ m² were analyzed. For all quantifications, three to six images were quantified per mouse, and data were plotted using GraphPad Prism.

Toluidine Blue Staining and Quantification. Perfused brain sections 30- μ m thick were mounted onto slides, outlined with a Pap pen, and washed with PBS before incubating in 2% Toluidine blue in PBS for ~5 min. Sections were monitored under a dissection microscope until PCs were adequately labeled. Slides were then washed in PBS until residual stain was removed, then allowed to dry before coverslipping with Permount. Sections were imaged on an Olympus microscope and PC counts were quantified by a blinded observer in ImageJ. The total number of PCs across a 200- μ m distance was quantified.

Luciferase Reporter Assay. HeLa cells were plated at 7.5×10^4 cells per well 24 h prior to transfection. Cells were transfected with 10-ng TOP or FOP flash, 1-ng *Renilla*, and 100 ng of gene of interest. For Wnt3a conditioned media, 24 h later media was changed and incubated overnight. Luciferase activity was measured 48 h posttransfection (Dual luciferase, Promega).

Coaffinity Purification. HeLa cells were plated at 0.5 to 1×10^6 cells per well 24 h prior to transfection, maintained in a 37 °C, 5.5% CO₂ incubator. When 70 to 80% confluent, cells were transfected with 0.5 μ g of gene of interest, 1 μ g of GST-ATXN1 plasmid, 4.5 μ g polyethylenimine (PEI), and Opti-MEM. Forty-eight hours posttransfection, cells were transferred into 1 mL PBS and centrifuged for 1 min at 13,000 rpm. The cells were resuspended in Triple lysis buffer, and rotated at 4 °C for 30 min to lyse cells. Cells were centrifuged for 15 min at 13,000 rpm at 4 °C. Supernatant was either kept for crude extract, or transferred to 20 μ L of washed glutathione-sepharose 4B beads (Millipore Sigma, GE17-0756-01) for affinity purification. Affinity purification samples were rotated overnight at 4 °C and washed five times in lysis buffer. All samples were diluted in 4 \times buffer with BME, and boiled for 10 min at 95 °C prior to loading gel. Western blots were run as described above. The following primary antibodies were used: T7 (Novagen 69522; 1:10,000), HA (Abcam ab91110; 1:5,000), c-Myc (Sigma M5546 clone 9e10; 1:1,000), β -catenin (BD 610154; 1:20,000), and GST (Sigma G7781; 1:3,000). To visualize GST signal, membranes were stripped with 10 mM sodium azide in TBST for 1 h, washed three times with TBST for 10 min each, and blocked with 5% nonfat milk in TBST for 1 h, prior to incubation with GST primary antibody overnight at 4 °C. Subsequent steps were performed as described above.

Mouse Behavioral Analysis. All behavioral studies were approved by the Yale University Institutional Animal Care and Use Committee. Mice were assessed for gait impairment and motor coordination using an accelerating rotating rod, dowel rod, and wire hang, as described previously (65–67). Investigators were blinded to mouse genotype. For all behavioral studies, mice were habituated to the behavior room prior to testing. For accelerating rotarod, the initial speed was set to 4 rpm, gradually accelerated to 40 rpm over 5 min, and maintained at 40 rpm for an additional 5 min. Latency to fall was recorded. Mice were tested for four trials per day, separated by 30 min, over 4 d. For both wire hang and dowel rod walking analyses, mice were placed at the center of either wire or a 9-mm dowel connected to platforms on either side, and time to first side touch of the adjacent platform, as well as total number of side touches in 120 s, was recorded.

Statistical Analysis. All statistical analyses were performed in GraphPad Prism. Data are shown as mean \pm SEM. To determine statistical significance, either two-tailed unpaired Student's *t* tests (when comparing two experimental groups) or one-way ANOVA with Tukey's post hoc analysis (when comparing more than two experimental groups) were performed, with a significance cutoff of $P < 0.05$. For rotarod behavioral analyses, a two-way ANOVA with Tukey's post hoc analysis was performed, with a significance cutoff of $P < 0.05$.

Data, Materials, and Software Availability. All study data are included in the main text and *SI Appendix*.

ACKNOWLEDGMENTS. We thank all members from the J.L. laboratory for technical support, thoughtful discussion, comments, and critiques for this project.

Signaling pathway schematics were created with BioRender. This work was supported by NIH Grants AG076154 (to J.L.), AG074609 (to J.L.), AG066447 (to J.L.), NS083706 (to J.L.), NS088321 (to J.L.), MH119803 (to J.L.), and T32 NS007224 (to K.L.); and the Lo Graduate Fellowship for Excellence in Stem Cell Research (to K.L. and L.T.).

Author affiliations: ^aInterdepartmental Neuroscience Program, Yale School of Medicine, New Haven, CT 06510; ^bDepartment of Neuroscience, Yale School of Medicine, New Haven, CT 06510; ^cDepartment of Genetics, Yale School of Medicine, New Haven, CT 06510; ^dDepartment of Neurology, Northwestern University Feinberg School of Medicine, Chicago, IL 60611; ^eYale College, New Haven, CT 06510; ^fProgram in Cellular Neuroscience, Neurodegeneration, and Repair, Yale School of Medicine, New Haven, CT 06510; and ^gYale Stem Cell Center, Yale School of Medicine, New Haven, CT 06510

- H. T. Orr *et al.*, Expansion of an unstable trinucleotide CAG repeat in spinocerebellar ataxia type 1. *Nat. Genet.* **4**, 221–226 (1993).
- H. T. Orr, H. Y. Zoghbi, SCA1 molecular genetics: A history of a 13 year collaboration against glutamines. *Hum. Mol. Genet.* **10**, 2307–2311 (2001).
- T. M. Driessen, P. J. Lee, J. Lim, Molecular pathway analysis towards understanding tissue vulnerability in spinocerebellar ataxia type 1. *eLife* **7**, e39981 (2018).
- H. G. Serra *et al.*, ROR α -mediated Purkinje cell development determines disease severity in adult SCA1 mice. *Cell* **127**, 697–708 (2006).
- C. R. Edamakanti, J. Do, A. Didonna, M. Martina, P. Opal, Mutant ataxin1 disrupts cerebellar development in spinocerebellar ataxia type 1. *J. Clin. Invest.* **128**, 2252–2265 (2018).
- X. Lin, B. Antalffy, D. Kang, H. T. Orr, H. Y. Zoghbi, Polyglutamine expansion down-regulates specific neuronal genes before pathologic changes in SCA1. *Nat. Neurosci.* **3**, 157–163 (2000).
- C. Ruegsegger *et al.*, Impaired mTORC1-dependent expression of homer-3 influences SCA1 pathophysiology. *Neuron* **89**, 129–146 (2016).
- M. Ingram *et al.*, Cerebellar transcriptome profiles of ATXN1 transgenic mice reveal SCA1 disease progression and protection pathways. *Neuron* **89**, 1194–1207 (2016).
- E. S. Lein *et al.*, Genome-wide atlas of gene expression in the adult mouse brain. *Nature* **445**, 168–176 (2007).
- A. Servadio *et al.*, Expression analysis of the ataxin-1 protein in tissues from normal and spinocerebellar ataxia type 1 individuals. *Nat. Genet.* **10**, 94–98 (1995).
- Y. Zhang *et al.*, An RNA-sequencing transcriptome and splicing database of glia, neurons, and vascular cells of the cerebral cortex. *J. Neurosci.* **34**, 11929–11947 (2014).
- K. R. Thomas, T. S. Musci, P. E. Neumann, M. R. Capecchi, W. Swaying is a mutant allele of the proto-oncogene *Wnt-1*. *Cell* **67**, 969–976 (1991).
- R. Goold *et al.*, Down-regulation of the dopamine receptor D2 in mice lacking ataxin 1. *Hum. Mol. Genet.* **16**, 2122–2134 (2007).
- L. Zeng *et al.*, Loss of the spinocerebellar ataxia type 3 disease protein ATXN3 alters transcription of multiple signal transduction pathways. *PLoS One* **13**, e0204438 (2018).
- Y. Komiya, R. Habas, Wnt signal transduction pathways. *Organogenesis* **4**, 68–75 (2008).
- A. Patapoutian, L. F. Reichardt, Roles of Wnt proteins in neural development and maintenance. *Curr. Opin. Neurobiol.* **10**, 392–399 (2000).
- V. Brault *et al.*, Inactivation of the beta-catenin gene by *Wnt1-Cre*-mediated deletion results in dramatic brain malformation and failure of craniofacial development. *Development* **128**, 1253–1264 (2001).
- H. J. Selvadurai, J. O. Mason, Activation of Wnt/ β -catenin signalling affects differentiation of cells arising from the cerebellar ventricular zone. *PLoS One* **7**, e42572 (2012).
- A. C. Hall, F. R. Lucas, P. C. Salinas, Axonal remodeling and synaptic differentiation in the cerebellum is regulated by WNT-7a signaling. *Cell* **100**, 525–535 (2000).
- Y. Pei *et al.*, WNT signaling increases proliferation and impairs differentiation of stem cells in the developing cerebellum. *Development* **139**, 1724–1733 (2012).
- A. Lorenz *et al.*, Severe alterations of cerebellar cortical development after constitutive activation of Wnt signaling in granule neuron precursors. *Mol. Cell. Biol.* **31**, 3326–3338 (2011).
- X. Wang, T. Imura, M. V. Sofroniew, S. Fushiki, Loss of adenomatous polyposis coli in Bergmann glia disrupts their unique architecture and leads to cell nonautonomous neurodegeneration of cerebellar Purkinje neurons. *Glia* **59**, 857–868 (2011).
- U. Schüller, D. H. Rowitch, Beta-catenin function is required for cerebellar morphogenesis. *Brain Res.* **1140**, 161–169 (2007).
- J. S. Brakeman, S. H. Gu, X. B. Wang, G. Dolin, J. M. Baraban, Neuronal localization of the adenomatous polyposis coli tumor suppressor protein. *Neuroscience* **91**, 661–672 (1999).
- J. Coyle-Rink, L. Del Valle, T. Sweet, K. Khalili, S. Amini, Developmental expression of Wnt signaling factors in mouse brain. *Cancer Biol. Ther.* **1**, 640–645 (2002).
- K. Watase *et al.*, A long CAG repeat in the mouse *Sca1* locus replicates SCA1 features and reveals the impact of protein solubility on selective neurodegeneration. *Neuron* **34**, 905–919 (2002).
- J. D. Fryer *et al.*, Exercise and genetic rescue of SCA1 via the transcriptional repressor *Capicua*. *Science* **334**, 690–693 (2011).
- P. Jafar-Nejad, C. S. Ward, R. Richman, H. T. Orr, H. Y. Zoghbi, Regional rescue of spinocerebellar ataxia type 1 phenotypes by 14-3-3 ϵ haploinsufficiency in mice underscores complex pathogenicity in neurodegeneration. *Proc. Natl. Acad. Sci. U.S.A.* **108**, 2142–2147 (2011).
- A. Ferrer-Vaquer *et al.*, A sensitive and bright single-cell resolution live imaging reporter of Wnt/ β -catenin signaling in the mouse. *BMC Dev. Biol.* **10**, 121–121 (2010).
- J. Friedrich *et al.*, Antisense oligonucleotide-mediated ataxin-1 reduction prolongs survival in SCA1 mice and reveals disease-associated transcriptome profiles. *JCI Insight* **3**, e123193 (2018).
- M. T. Veeman, D. C. Slusarski, A. Kaykas, S. H. Louie, R. T. Moon, Zebrafish prickle, a modulator of noncanonical Wnt/*Fz* signaling, regulates gastrulation movements. *Curr. Biol.* **13**, 680–685 (2003).
- B. T. MacDonald, K. Tamai, X. He, Wnt/ β -catenin signaling: Components, mechanisms, and diseases. *Dev. Cell* **17**, 9–26 (2009).
- L. Tejwani, J. Lim, Pathogenic mechanisms underlying spinocerebellar ataxia type 1. *Cell. Mol. Life Sci.* **77**, 4015–4029 (2020).
- H. Y. Zoghbi, H. T. Orr, Pathogenic mechanisms of a polyglutamine-mediated neurodegenerative disease, spinocerebellar ataxia type 1. *J. Biol. Chem.* **284**, 7425–7429 (2009).
- E. N. Burchright *et al.*, SCA1 transgenic mice: A model for neurodegeneration caused by an expanded CAG trinucleotide repeat. *Cell* **82**, 937–948 (1995).
- J. Grosche *et al.*, Microdomains for neuron-glia interaction: Parallel fiber signaling to Bergmann glial cells. *Nat. Neurosci.* **2**, 139–143 (1999).
- K. Yamada *et al.*, Dynamic transformation of Bergmann glial fibers proceeds in correlation with dendritic outgrowth and synapse formation of cerebellar Purkinje cells. *J. Comp. Neurol.* **418**, 106–120 (2000).
- S. K. Custer *et al.*, Bergmann glia expression of polyglutamine-expanded ataxin-7 produces neurodegeneration by impairing glutamate transport. *Nat. Neurosci.* **9**, 1302–1311 (2006).
- M. Cvetanovic, Decreased expression of glutamate transporter GLAST in Bergmann glia is associated with the loss of Purkinje neurons in the spinocerebellar ataxia type 1. *Cerebellum* **14**, 8–11 (2015).
- M. Cvetanovic, M. Ingram, H. Orr, P. Opal, Early activation of microglia and astrocytes in mouse models of spinocerebellar ataxia type 1. *Neuroscience* **289**, 289–299 (2015).
- A. Buffo, F. Rossi, Origin, lineage and function of cerebellar glia. *Prog. Neurobiol.* **109**, 42–63 (2013).
- T. C. Bellamy, Interactions between Purkinje neurones and Bergmann glia. *Cerebellum* **5**, 116–126 (2006).
- C. I. De Zeeuw, T. M. Hoogland, Reappraisal of Bergmann glial cells as modulators of cerebellar circuit function. *Front. Cell. Neurosci.* **9**, 246 (2015).
- T. Sasaki *et al.*, Application of an optogenetic byway for perturbing neuronal activity via glial photostimulation. *Proc. Natl. Acad. Sci. U.S.A.* **109**, 20720–20725 (2012).
- K. Yamada, M. Watanabe, Cytodifferentiation of Bergmann glia and its relationship with Purkinje cells. *Anat. Sci. Int.* **77**, 94–108 (2002).
- F. Alliot, B. Pessac, Astrocytic cell clones derived from established cultures of 8-day postnatal mouse cerebella. *Brain Res.* **306**, 283–291 (1984).
- K. J. Robinson, M. Watchon, A. S. Laird, Aberrant cerebellar circuitry in the spinocerebellar ataxias. *Front. Neurosci.* **14**, 707 (2020).
- J. H. Kim, A. Lukowicz, W. Qu, A. Johnson, M. Cvetanovic, Astroglia contribute to the pathogenesis of spinocerebellar ataxia type 1 (SCA1) in a biphasic, stage-of-disease specific manner. *Glia* **66**, 1972–1987 (2018).
- B. Ma, M. O. Hottiger, Crosstalk between Wnt/ β -catenin and NF- κ B signaling pathway during inflammation. *Front. Immunol.* **7**, 378 (2016).
- N. C. Inestrosa, L. Varela-Nallar, C. P. Grabowski, M. Colombres, Synaptotoxicity in Alzheimer's disease: The Wnt signaling pathway as a molecular target. *UBMB Life* **59**, 316–321 (2007).
- E. M. Toledo, N. C. Inestrosa, Activation of Wnt signaling by lithium and rosiglitazone reduced spatial memory impairment and neurodegeneration in brains of an APP^{swe}/PSEN1 Δ E9 mouse model of Alzheimer's disease. *Mol. Psychiatry* **15**, 272–285, 228 (2010).
- A. R. Alvarez *et al.*, Wnt-3a overcomes beta-amyloid toxicity in rat hippocampal neurons. *Exp. Cell Res.* **297**, 186–196 (2004).
- O. A. da Cruz e Silva, A. G. Henriques, S. C. Domingues, E. F. da Cruz e Silva, Wnt signalling is a relevant pathway contributing to amyloid β -peptide-mediated neuropathology in Alzheimer's disease. *CNS Neurol. Disord. Drug Targets* **9**, 720–726 (2010).
- B. Li *et al.*, WNT5A signaling contributes to $\text{A}\beta$ -induced neuroinflammation and neurotoxicity. *PLoS One* **6**, e22920 (2011).
- Y. Chen *et al.*, Wnt signaling pathway is involved in the pathogenesis of amyotrophic lateral sclerosis in adult transgenic mice. *Neurosci. Res.* **34**, 390–399 (2012).
- Y. Chen *et al.*, Activation of the Wnt/ β -catenin signaling pathway is associated with glial proliferation in the adult spinal cord of ALS transgenic mice. *Biochem. Biophys. Res. Commun.* **420**, 397–403 (2012).
- J. D. Godin, G. Poizat, M. A. Hickey, F. Maschat, S. Humbert, Mutant huntingtin-impaired degradation of beta-catenin causes neurotoxicity in Huntington's disease. *EMBO J.* **29**, 2433–2445 (2010).
- P. C. Marcogliese *et al.*, Loss of IRF2BPL impairs neuronal maintenance through excess Wnt signaling. *Sci. Adv.* **8**, eabl5613 (2022).
- N. C. Inestrosa, L. Varela-Nallar, Wnt signaling in the nervous system and in Alzheimer's disease. *J. Mol. Cell Biol.* **6**, 64–74 (2014).
- P. Polakis, Wnt signaling in cancer. *Cold Spring Harb. Perspect. Biol.* **4**, a008052 (2012).
- T. Zhan, N. Rindtorff, M. Boutros, Wnt signaling in cancer. *Oncogene* **36**, 1461–1473 (2017).
- A. R. Kang, H. T. An, J. Ko, S. Kang, Ataxin-1 regulates epithelial-mesenchymal transition of cervical cancer cells. *Oncotarget* **8**, 18248–18259 (2017).
- G. Coarelli *et al.*, Low cancer prevalence in polyglutamine expansion diseases. *Neurology* **88**, 1114–1119 (2017).
- A. E. Murrmann, J. Yu, P. Opal, M. E. Peter, Trinucleotide repeat expansion diseases, RNAi, and cancer. *Trends Cancer* **4**, 684–700 (2018).
- J. Lim *et al.*, Opposing effects of polyglutamine expansion on native protein complexes contribute to SCA1. *Nature* **452**, 713–718 (2008).
- J. Crespo-Barreto, J. D. Fryer, C. A. Shaw, H. T. Orr, H. Y. Zoghbi, Partial loss of ataxin-1 function contributes to transcriptional dysregulation in spinocerebellar ataxia type 1 pathogenesis. *PLoS Genet.* **6**, e1001021 (2010).
- H. Ju *et al.*, Polyglutamine disease toxicity is regulated by Nemo-like kinase in spinocerebellar ataxia type 1. *J. Neurosci.* **33**, 9328–9336 (2013).